Increased Light Extraction from GaN Light-Emitting Diodes by SiN_X Compound Eyes

Eun Kyu Kang, Young Min Song, Sung Jun Jang, Chan Il Yeo, and Yong Tak Lee

***Abstract*— We demonstrate GaN-based blue light-emitting diodes (GaN LEDs) with artificial compound eye structures (CESs). The GaN LEDs consist of microlens arrays (MLAs) and antireflective subwavelength structures (SWSs). The CESs, formed on the LED surface by two-step pattern transfer of reflowed photoresist micro patterns and Ag nanoparticles, play an important role in enhancing the light extraction efficiency by reducing both the Fresnel and the total internal reflection. The CES integrated GaN LEDs show an output power enhancement of 93% compared to that of conventional GaN LEDs with flat surface, without any serious degradation of electrical characteristics. Optical simulations by ray-tracing and the rigorous coupled-wave analysis method provide design guidelines for MLAs and SWSs, respectively.**

***Index Terms*— GaN-based LEDs, light extraction efficiency, microlens, subwavelength structure, compound eye structures.**

I. Introduction

HIERARCHICAL micro/nanostructures in nature provide many interesting useful functions, such as the outstanding adhesion of gecko toes [1], the super hydrophobic wetting property of lotus leaves [2], and the antireflection property of nipple arrays in the compound eyes of moths [3], [4]. Among them, compound eyes are very useful in various optical industries because they have broadband and omnidirectional antireflection properties [5]. Compound eyes consist of subwavelength structures (SWSs) with tapered profiles on hexagonal microlens arrays (MLAs). In nature, surfaces with SWSs behave as graded reflective index media that have the impressive effect of reducing the Fresnel reflection (FR) [6] by providing refractive index matching at the interface between air and the lens. On the other hand, MLAs effectively collect omnidirectional incident light, and the collected light is directed towards the photoreceptor cells [4]. These two functional structures can be directly used to enhance light extraction efficiencies in light-emitting materials/devices. In other words, SWSs and MLAs reduce the Fresnel loss and the total internal reflection (TIR) loss, respectively, at the interface between two different optical media. An initial demonstration of bio-inspired compound eye structures (CESs) on GaP-based red LEDs showed excellent performance for light extraction efficiency [8]. Previously, the large index-contrast embedded photonic crystals [9], [10], self-assembled colloidal MLAs [11], [12], [14], and concave microstructure arrays via imprinting methods [13] had been used for achieving improved light extraction over a large angular distribution, which in turn resulted in significant increase in light extraction efficiency in GaN-based LEDs (GaN LEDs). Similar concept by using colloidal MLAs had also been used for efficient extraction of both guided mode and substrate mode in organic LED [14]. However, GaN LEDs with CESs have not yet been reported despite their important functionalities [15].

In this letter, we demonstrate GaN LEDs with artificial CESs, in which GaN LEDs consist of hemispherical MLAs and tapered SWSs formed by using a combination of thermal reflow and dewetting processes. Also, optical simulations using ray-tracing and rigorous coupled-wave analysis (RCWA) methods were conducted to provide design guidelines for MLAs and SWSs, respectively.

II. Device Structure and Fabrication

A schematic diagram of the fabrication steps of CESs on conventional GaN LED is given in Fig. 1. Blue InGaN/GaN LED (λ = 460 nm) were grown on a c-plane non-patterned double side polished sapphire (Al_2O_3) substrate using metal-organic chemical vapor deposition system. The epitaxial structure consisted of an un-doped GaN buffer layer (1.3 μm), Si-doped n-type GaN layer (5 μm), heavily Si-doped n-type GaN layer (1.3 μm), five-periods of InGaN (well)/GaN (barrier) multiple-quantum–wells, and Mg-doped p-type GaN layer (100 nm). First, conventional GaN LEDs with an indium-tin-oxide (ITO) contact layers (150 nm) were prepared using a standard process, as follows: using conventional photolithography process and BCl_2/Cl_2 inductive coupled plasma etching process, the LED wafer was partially etched to form a mesa (400 μm $\times$ 400 μm) until the exposed n-type GaN layer was approximately 700 nm thick. Then, a 150 nm thick ITO layer was deposited on the top of the p-GaN layer using an e-beam evaporator and the sample was annealed using a rapid thermal annealing (RTA) system. In order to serve as p- and n-metal contacts, Ni/Au (30/300 nm) and Ti/Al/Ti/Au (30/80/30/300 nm) metals were then deposited respectively, using an e-beam evaporator.

Manuscript received March 5, 2013; revised April 2, 2013 and April 7, 2013; accepted April 8, 2013. Date of publication May 1, 2013; date of current version May 24, 2013. This work was supported in part by the Technology Innovation Program of the Ministry of Knowledge Economy under Grant 2007-F-045-03.

E. K. Kang, Y. M. Song, S. J. Jang, and C. I. Yeo are with the School of Information and Communications, Gwangju Institute of Science and Technology, Gwangju 500-712, Korea (e-mail: ekkang@gist.ac.kr; ymsong81@gmail.com; sung.jang@northwestern.edu; ciyeo@gist.ac.kr).

Y. T. Lee is with the School of Information and Communications, Gwangju Institute of Science and Technology, Gwangju 500-712, Korea, and also with the Department of Nanobio Materials and Electronics, Gwangju Institute of Science and Technology, Gwangju 500-712, Korea (e-mail: ytlee@gist.ac.kr).

Color versions of one or more of the figures in this letter are available online at http://ieeexplore.ieee.org.

Digital Object Identifier 10.1109/LPT.2013.2260324

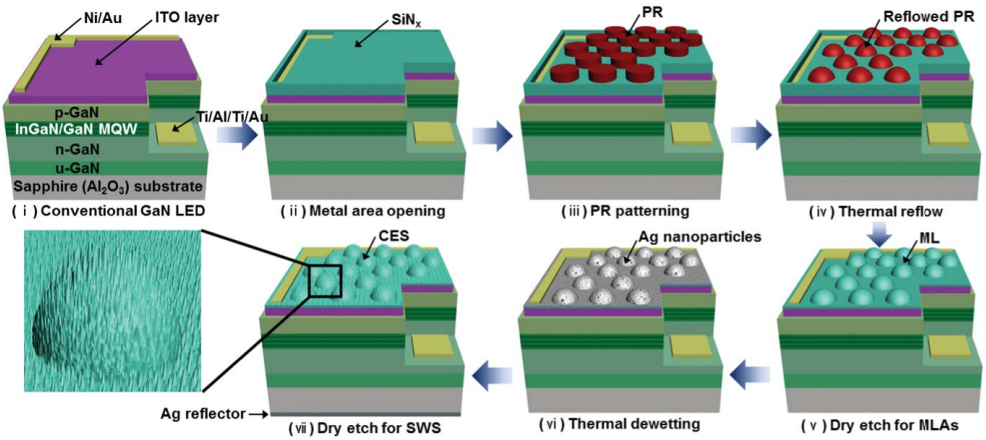

Fig. 1. Schematic illustration of the fabrication process for GaN LED with CESs.

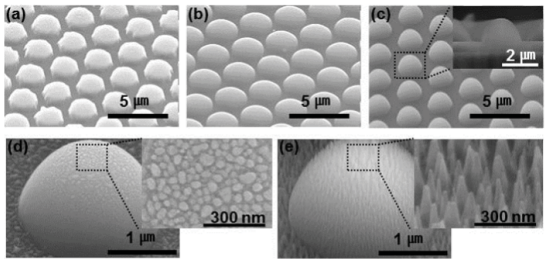

Fig. 2. SEM images of SiN_x surface at each fabrication step for integration of CESs: (a) cylindrical PR patterns, (b) lens-like PR patterns after thermalreflow, (c) MLAs on the SiN_x layer after dry etching, (d) Ag nanoparticles on MLs and surface, and (e) integrated CESs.

For the fabrication of CESs on conventional GaN LEDs, first, a 10 nm thick SiO_2 interlayer was deposited on the top surface of the LEDs using RF magnetron sputtering system. The SiO_2 interlayer prevents hydrogen plasma damage of the ITO layer, which generally occurs in plasma enhanced chemical vapor deposition system [16]. Then, a 2 μm thick SiN_x layer was deposited onto ITO layer. This was because the usual thickness (100–500 nm) [17] of a p-type GaN layer is inadequate for the fabrication of CESs. Also, SiN_x has a refractive index similar to that of ITO, and is transparent over the entire visible wavelength range [18].

An array of hemispherical photoresist (PR) patterns with a diameter of 2 μm, as shown Fig. 2 (b), formed by conventional photolithography and subsequent thermal reflow process, was used as an etch mask to fabricate SiN_x MLAs of height 1.3 μm generated by pattern transfer process with reactive ion etching (RIE) at optimum conditions, i.e., CF_4 (30 sccm) with rf power of 100 W for 20 min (Fig. 2 (c)).

To integrate the SWSs on the MLAs, a 10 nm thick Ag film was deposited using an e-beam evaporator. Then, thermal dewetting of Ag thin film [8] was carried out to form Ag nanoparticles with a RTA process at 400 °C for 60 s in nitrogen ambient, as shown Fig. 2 (d). Ag nanoparticles are randomly distributed, however, over a large area, Ag nanoparticles are uniformly distributed. The average distance and size of Ag nanoparticles can be easily controlled by adjusting the thickness of Ag films and annealing temperature [6]. The dewetting temperature was carefully chosen to avoid peeling of the SiN_x layer originating from the thermal expansion coefficient mismatch of ITO (7.2×10^{-6} / °C) and SiN_x (3.27×10^{-6} / °C) [19], [20].

To form SiN_x SWS with a tapered profile as shown in Fig. 2 (e), the underlying SiN_x layer was etched using RIE in CF_4 ambient. The residual Ag mask was removed with Au etchant (I_2 0.09 mol/l, KI 0.6 mol/l). Finally, a 1 μm thick Ag film was deposited on the back side of the polished sapphire of all the fabricated GaN LEDs for further enhancement of light extraction.

III. Simulation Result and Characteristics

The geometry of the MLAs and the period of the SWSs with tapered profile play major roles in light extraction. Hence, it was necessary to calculate the TIR and FR according to the geometry of the MLAs and the period of the SWS in order to determine the optimal height of the MLAs and the period of the SWS, respectively. In the case of the calculation of the TIR by ray tracing [21], the model used in this calculation was constructed for SiN_x MLAs with diameters of 2 μm and separation lengths of 1 μm, whose valves were determined according to the height of MLAs. Fig. 3 (a) shows the light extraction efficiency of the MLAs integrated GaN LED (MLA GaN LED) as a function of the height of the MLAs at the emission wavelength of 460 nm. Light extraction efficiency of the flat surface and the MLAs formed surface with a height of 1 μm, which was similar to a surface of hemispherical MLAs, gave values of 20% and 37.2%, respectively.

In the case of the flat surface, the generated omnidirectional light from the active region cannot escape from the GaN LED when the incident angle exceeds the critical angle. On the other hand, the hemispherical MLAs formed on the surface of the GaN LED can maximally extricate the light at angles over the critical angle, owing to the changed incident light angle at the interface between the air and the SiN_x MLAs.

In the case of the calculation of FR by RCWA [6], the model used in this calculation was constructed for a SiN_x SWS with a tapered profile on a GaN/ITO substrate, as shown in the inset of Fig. 3 (b). In this calculation, the reflectance from

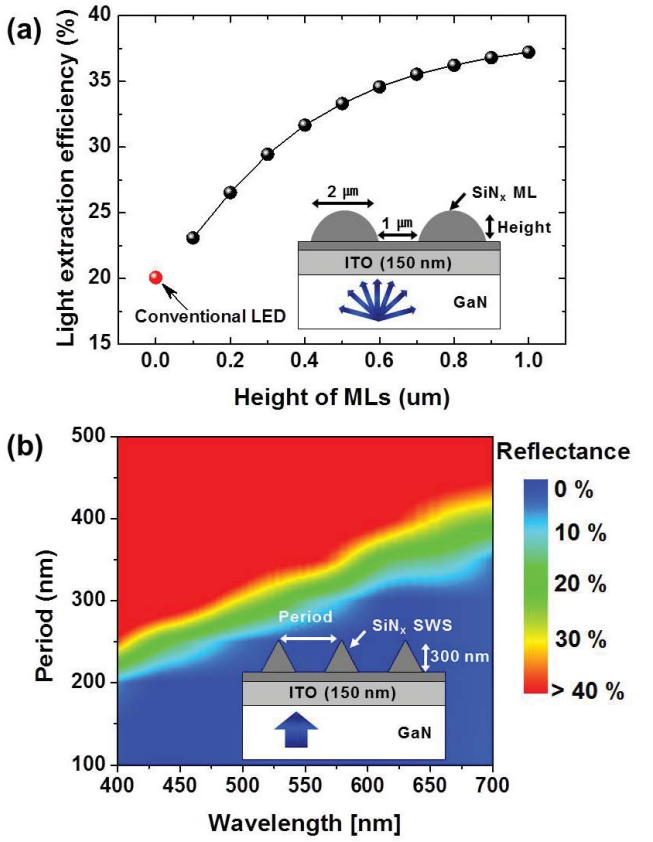

Fig. 3. (a) Simulated light extraction efficiency as a function of height of SiN_X MLAs (black symbols) and conventional LED (red symbol). (b) Contour plot of the calculated reflectance as a function of the period of SiN_X SWSs on ITO/GaN substrate and incident wavelength.

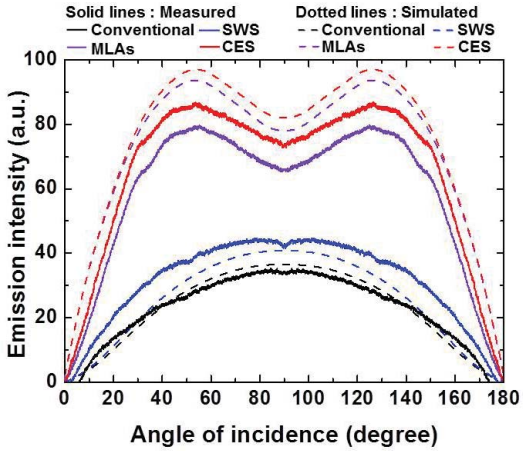

Fig. 4. The measured and simulated far-field emission patterns of various GaN LEDs.

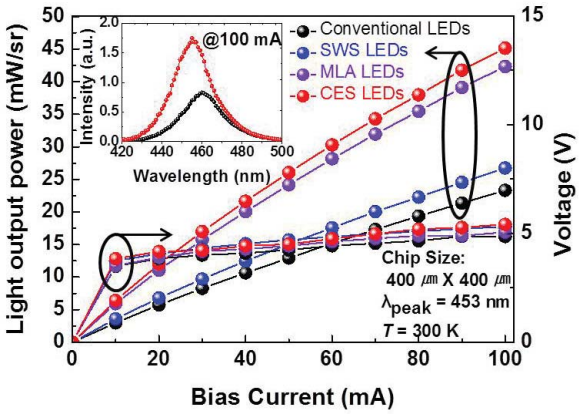

Fig. 5. L-I-V of conventional and textured GaN LEDs with Ag reflector as a function of injection current. The inserted figure shows the EL spectra of conventional LEDs and CES GaN LEDs; the bias current was 100 mA.

the interface between GaN, ITO, and SiN_X was taken in to account. Fig. 3 (b) shows the contour plot of the reflectance variation caused by the internal reflection as a function of the SWS period and the incident wavelength. At an incident wavelength of 460 nm, the SWS with a period of >250 nm exhibited very high reflectance (>20%) due to higher order diffraction [6]. According to the simulations, the period of the SWS with the tapered profile should be shorter than ~200 nm in order to reduce the higher order diffraction at the operating wavelength.

In order to further investigate the significant difference of the far-field emission patterns of various GaN LEDs, the far-field emission patterns of various GaN LEDs were simulated using ray-tracing and measured using a goniometer.

The far-field measurements were taken from $\theta = 0°$ up to $\theta = 90°$ and results for the $\theta = 90°-180°$ range are identical to those from the $\theta = 0°-90°$ range. Fig. 4 shows the simulated (dotted) and the measured (solid) far-field emission patterns of the various GaN LEDs. In the simulation, SWS refers to an effective single medium that has a refractive index (n) of 1.54 and a thickness of $\lambda/4n$. In the case of far-field emission pattern of SWS integrated GaN LEDs (SWS GaN LEDs), Lambetian-like patterns similar to those of conventional GaN LEDs can be observed, however, the emission intensity is stronger than that of conventional GaN LEDs at all angles due to the reduction of FR to the level of the critical angle. The far-field emission patterns of the MLA GaN LEDs and the CES integrated LEDs (CES GaN LEDs) show considerably stronger level of emission intensity at all angles compared to that of conventional GaN LEDs. The emission patterns are totally different in comparison to those of conventional GaN LEDs, especially, at an angle of around 50°. These results are attributed to the formation of MLAs, which is thought to increase the effective critical angle [22]. In addition, the emission intensity of CES GaN LEDs showed the highest emission intensity at all range of angles studied due to the reduction of both FR and TIR. The present simulation studies were intended to provide the trend of the experiments. Recent works had clarified on the accurate model for simulating the LED with surface roughened surface [23], and the use of 3-D FDTD modeling is required for accurate simulation of the GaN LEDs with MLAs [24]. Prior works based on 3-D FDTD had also shown that the use of MLAs resulted in large increase in the light extraction at large angular distribution [24].

Light-output power from the LEDs was measured in the normal direction. Fig. 5 plots the light-output power and the voltage as functions of the bias current for the four fabricated types of LED. Compared to conventional GaN LEDs, all textured-GaN LEDs showed enhanced light-output characteristics

without serious degradation of the electrical characteristics. These results prove the effects of SWSs and MLAs on the enhancement of light extraction. Among the fabricated GaN LEDs, the SWS GaN LEDs showed an enhancement ratio about 14.5% on account of the reduction of the FR; MLA GaN LEDs showed an approximately 81.5% on account of the reduction of the TIR. Compared to the conventional GaN LEDs, the CES GaN LEDs showed the highest enhancement ratio of about 93.5% due to the reduction of both the FR and TIR, at a bias current of 100 mA. In the case of EL spectra, in comparison with the conventional GaN LEDs, the blue shift of the peak wavelength of the CES GaN LEDs was approximately 5 nm due to the increase in the junction temperature [25]. The SiN_x layer makes it slightly difficult to accomplish thermal dissipation in GaN LEDs. However, except for the small blue shift, these results certainly show that SiN_x CESs can efficiently reduce FR and TIR in GaN LEDs thereby increasing the light output.

IV. Conclusion

We have optimized SWS period and MLA shape through theoretical calculation, and for the improvement of the light extraction efficiency, CESs were fabricated onto conventional GaN LEDs based on simulation results by using simple fabrication methods such as thermal reflow of PR and thermal dewetting process of Ag film. The CESs GaN LEDs showed a 93.5% enhancement in light extraction efficiency over that of conventional GaN LEDs without any serious degradation of the electrical characteristics. This fabrication method can be applied for the light output enhancement of GaN LEDs emitting at ultraviolet and green wavelengths. These results show the promise of CESs GaN LEDs in realizing low-cost and high efficiency solid-state lighting.

References

[1] K. Autumn, "How gecko toes stick," *Amer. Sci.*, vol. 94, no. 2, p. 124, Mar./Apr. 2006.

[2] L. Feng, *et al.*, "Super-hydrophobic surface: From natural to artificial," *Adv. Mater.*, vol. 14, no. 24, pp. 1857–1860, Dec. 2002.

[3] D. G. Stavenga, S. Foletti, G. Palasantzas, and K. Arikawa, "Light on the moth-eye corneal nipple array of butterflies," *Proc. Biol. Sci.*, vol. 273 no. 1587, pp. 661–667, Mar. 2006.

[4] L. P. Lee and R. Szema, "Inspirations from biological optics for advanced photonic systems," *Science*, vol. 310, no. 5751, pp. 1148–1150, Nov. 2005.

[5] H. J. Jung and K. H. Jeong, "Monolithic polymer microlens arrays with antireflective nanostructures," *Appl. Phys. Lett.*, vol. 101, no. 20, pp. 203102-1–203102-4, Nov. 2012.

[6] Y. M. Song, E. S. Choi, G. C. Park, C. Y. Park, S. J. Jang, and Y. T. Lee, "Disordered antireflection nanostructures on GaN-based light-emitting diodes using Ag nanoparticles for improved light extraction efficiency," *Appl. Phys. Lett.*, vol. 97, no. 9, pp. 093110-1–093110-3, Sep. 2010.

[7] E. J. Hong, K. J. Byeon, H. W. Park, J. Y. H. Lee, K. W. Choi, and G. Y. Jung, "Fabrication of moth-eye structure on p-GaN layer of GaN-based LEDs for improvement of light extraction," *Mater. Sci. Eng., B*, vol. 163, no. 3, pp. 170–173, Jul. 2009.

[8] Y. M. Song, G. C. Park, S. J. Jang, J. H. Ha, J. S. Yu, and Y. T. Lee, "Multifunctional light escaping architecture inspired by compound eye surface structures: From understanding to experimental demonstration," *Opt. Express*, vol. 19, no. S2, pp. A157–A165, Mar. 2011.

[9] E. Matioli, *et al.*, "High extraction efficiency GaN-based photonic-crystal light-emitting diodes: Comparison of extraction lengths between surface and embedded photonic crystals," *Appl. Phys. Express*, vol. 3, pp. 032103-1–032103-3, Mar. 2010.

[10] J. Jewell, *et al.*, "Double embedded photonic crystals for extraction of guided light in light-emitting diodes," *Appl. Phys. Lett.*, vol. 100, no. 17, pp. 171105-1–171105-4, Apr. 2012.

[11] Y. K. Ee, R. A. Arif, and N. Tansu, "Enhancement of light extraction efficiency of InGaN quantum wells light emitting diodes using SiO_2/polystyrene microlens arrays," *Appl. Phys. Lett.*, vol. 91, no. 16, pp. 221107-1–221107-3, Nov. 2007.

[12] X. H. Li, *et al.*, "Light extraction efficiency enhancement of III-nitride light-emitting diodes by using 2-D close-packed TiO_2 microsphere arrays," *J. Display Technol.*, vol. 9, no. 5, pp. 323–331, 2013.

[13] Y. K. Ee, P. Kumnorkaew, R. A. Arif, H. Tong, J. F. Gilchrist, and N. Tansu, "Light extraction efficiency enhancement of InGaN quantum wells light-emitting diodes with polydimethylsiloxane concave microstructures," *Opt. Express*, vol. 17, no. 16, pp. 13747–13757, Aug. 2009.

[14] W. H. Koo, W. Youn, P. Zhu, X. H. Li, N. Tansu, and F. So, "Light extraction of organic light emitting diodes by defective hexagonal-close-packed array," *Adv. Functional Mater.*, vol. 22, no. 16, pp. 3454–3459 Aug. 2012.

[15] H. S. Kim, *et al.*, "Unusual strategies for using indium gallium nitride grown on silicon (111) for solid-state lighting," *Proc. Nat. Acad. Sci.*, vol. 108, no. 25, pp. 10023–10372, Jun. 2011.

[16] B. J. Kim, *et al.*, "A study of oxygen reduction of Tin-or Zinc-doped indium oxide (ITO or IZO) film induced by deposition of silicon nitride film in PECVD process," *Mater. Res. Soc.*, vol. 936, no. 1, pp. 1–6, Jun. 2006.

[17] S. T. Li, *et al.*, "GaP single crystal layers grown on GaN by MOCVD," *Proc. SPIE*, vol. 7518, p. 75180F, Oct. 2009.

[18] Y. J. Lee, S. H. Kim, J. Huh, G. H. Kim, and Y. H. Lee, "A high-extraction-efficiency nanopatterned organic light-emitting diode," *Appl. Phys. Lett.*, vol. 82, no. 21, pp. 3779–3782, Apr. 2003.

[19] Y. C. Lin, W. Q. Shi, and Z. Z. Chen, "Effect of deflection on the mechanical and optoelectronic properties of indium tin oxide films deposited on polyethylene terephthalate substrates by pulse magnetron sputtering," *Thin Solid Films*, vol. 517, no. 5, pp. 1701–1705, Jan. 2009.

[20] C. L. Tien and T. W. Lin, "Thermal expansion coefficient and thermo-mechanical properties of SiN_x thin films prepared by plasma-enhanced chemical vapor deposition," *Appl. Opt.*, vol. 51, no. 30, pp. 7229–7235, Oct. 2012.

[21] J. K. Kim, *et al.*, "Elimination of total internal reflection in GaInN light-emitting diodes by graded-refractive-index micropillars," *Appl. Phys. Lett.*, vol. 93, no. 22, pp. 221111-1–221111-3, Dec. 2008.

[22] X. H. Li, R. B. Song, Y. K. Ee, P. Kumnokaew, J. F. Gilchrist, and N. Tansu, "Light extraction efficiency and radiation patterns of III-nitride light-emitting diodes with colloidal microlens arrays with various aspect ratios," *IEEE Photon. J.*, vol. 3, no. 3, pp. 489–499, Jun. 2011.

[23] A. David, "Surface-roughened light-emitting diodes: An accurate model," *J. Display Technol.*, vol. 9, no. 5, pp. 300–315, May 2013.

[24] P. F. Zhu, G. Liu, J. Zhang, and N. Tansu, "FDTD analysis on extraction efficiency of GaN light-emitting diodes with microsphere arrays," *J. Display Technol.*, vol. 9, no. 5, pp. 316–322, May 2013.

[25] S. Chhajed, *et al.*, "Junction temperature in light-emitting diodes assessed by different methods," *Proc. SPIE*, vol. 5739, pp. 16–24, Mar. 2005.